19th Brazilian Congress of Thermal Sciences and Engineering
November 06th-10th, 2022, Bento Gonçalves - RS - Brazil

ENC-2022-0240
NUMERICAL CHARACTERIZATION OF THE GEOMETRY AT THE ENTRANCE TO THE TANK IN THE FORMATION AND DEVELOPMENT OF THE GRAVITATIONAL VORTEX OF WATER

Roberto Carlos Chucuya Huallpachoque
Cesar Vallejo University, Engineering Faculty, Av. Central, Mz. H Lt. 1, Chimbote, Ancash, Perú.
rchucuya@ucv.edu.pe

Nicol Dayana Gonzalez Chonseng
National University of Santa, Engineering Faculty, Av. Universitaria S/N, Nuevo Chimbote, Ancash, Perú.
gonzchonnicol1997@gmail.com

Ursus Jhonatan Sandoval Vasquez
National University of Santa, Engineering Faculty, Av. Universitaria S/N, Nuevo Chimbote, Ancash, Perú.
Jsandovalv1796@gmail.com

Luis Fernando Junior Saldaña Bernuy
São Paulo State University, Guaratinguetá Engineering Faculty, Av. Ariberto P. Cunha, 333, Guaratinguetá, SP, CEP 12516-410, Brazil.
luis.bernuy@unesp.br

Abstract. *In Peru, the participation in the production of electric energy by means of mini-hydraulic energy (less than 20 MW) is 2.5% of the total generated, for this reason, it is important to conduct investigations to boost this low percentage of production. To address this circumstance, the use of vortex velocity in a gravitational vortex hydraulic energy generation system is presented as a potential alternative solution. The modeling of the geometry was carried out in Autodesk Inventor which is compatible with the ANSYS 2020 R1 software, whose dimensions were for both geometries the entrance is square of 1.5 m and a development length of 7.5 m, the diameter of the cylinder is 5.5 m and the discharge diameter of 1.0 m. The mesh used for the conical geometry was the MultiZone method and for the cylindrical geometry two types of mesh were performed, for the inlet channel and discharge cone the MultiZone method was used and for the cylindrical tank the Automatic method. The superficial flow velocities for the geometry of the conical and cylindrical tank are in the range of 2.26 m/s to 2.58 m/s and 1.85 m/s to 2.23 m/s, respectively, the latter does not present a well-behaved velocity field, being able to this generates instabilities in the operation of the turbine.*

Keywords: *gravitational vortex; cylindrical and conical inlet geometry; numerical modelling; Ansys 2021 R1.*

1. INTRODUCTION

Latin America has the potential to produce electricity from renewable sources, especially hydropower. Brazil, Ecuador and Peru are among the nine best producers of hydropower worldwide, where the vast majority are large-scale hydropower plants (Céspedes and Saldaña, 2021). In Peru, hydroelectric power plants, regardless of their capacity, have been covering the base of the electricity demand due to their low operating costs; however, demand peaks are covered by natural gas thermoelectric power plants with gas cycles. According to the report of the Economic Operation Committee of the COES System in Peru for the year 2020, electricity generation was 49,186 GWh, in which the participation in generation by hydroelectric plants was 59.60 %, thermoelectric plants generated 35.15 %, while wind and solar plants generated 3.67 and 1.58% respectively, adding the generation with Renewable Energy Resources (RER) which represented 5.25% (COES, 2020).

The hydroelectric power generation plants can be classified into many types where one of them is the micro hydroelectric power plant (Faraji et al., 2022), in this sense, the micro hydroelectric generation plants of gravitational vortex water are presented as a technology that favors electrical generation due to the simple form of its design and that in turn, it is compatible with low hydraulic jump (Edirisinghe et al., 2022). This technology can generate approximately

up to 10 KW of electrical power, are in the range of micro hydroelectric generation and can be sufficient for supplying small communities (Timilsina, Mulligan, & Bajracharya, 2018).

In its most general classification, it can be said that there are two types of vortices: the forced vortex and the free vortex (Gardea, 2001). The forced vortex Fig. 1 is the easiest to understand, since it is generated by the contact between a real fluid in motion and an obstacle that can be a fixed wall or another fluid whose velocity is contrary to that of the first one, or simply whose velocity is slightly different from that of the real fluid. The free vortex Fig. 2 typically occurs on a discharge that may be "bottom" as occurs in bath tubs or sinks when emptying, after the liquid was originally at rest. A similar case is that of the vortex formed due to the suction caused by a pump in a pipeline, or that which occurs in the intake works of dams (Arregui et al., 2017).

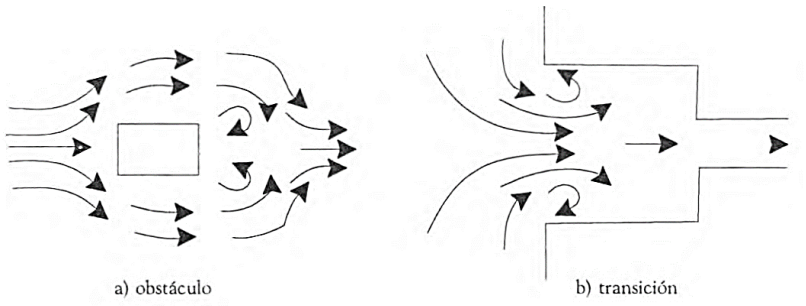

Figure 1. Vortices Forced by Obstacle (left) and Transition (right)

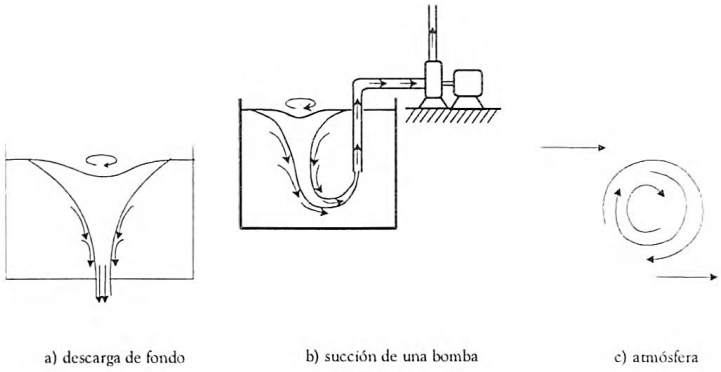

Figure 2. Free vortices by bottom discharge (left), pump suction (middle) and atmosphere (right).

2. DEVELOPMENT OF THE CFD MODEL

In this research, a parametric study was performed on the gravity vortex generation system to determine the configuration of the conical or cylindrical tank geometric system that generates the highest gravity water velocity, so that maximum power can be harnessed. This parametric study was carried out with ANSYS 2022R1 software.

The Navier-Stokes fluid dynamics equations form the basic theory of CFD modeling, which are used to model the flow parameters of a fluid, among which are velocity, temperature and pressure (Lopez, 2015). The general form of the Navier-Stokes equations in Cartesian coordinates for a compressible flow is:

Mass conservation equation:

$$\frac{\partial \rho}{\partial t} + \frac{\partial (\rho u)}{\partial x} + \frac{\partial (\rho v)}{\partial x} + \frac{\partial (\rho w)}{\partial x} = 0 \tag{1}$$

Where *u*, *v* and *w* are the velocity in the *x*, *y* and *z* direction respectively, and t is the time.

Equations of quantity of motion (momentum):

$$Mx: \frac{\partial (\rho u)}{\partial t} + u\frac{\partial (\rho u)}{\partial x} + v\frac{\partial (\rho u)}{\partial x} + w\frac{\partial (\rho u)}{\partial x} = -\frac{1}{\rho}\frac{\partial p}{\partial x} + v\frac{\partial^2 u}{\partial x^2} + v\frac{\partial^2 u}{\partial y^2} + v\frac{\partial^2 u}{\partial z^2} \tag{2}$$

$$My: \frac{\partial (\rho v)}{\partial t} + u\frac{\partial (\rho v)}{\partial x} + v\frac{\partial (\rho v)}{\partial x} + w\frac{\partial (\rho v)}{\partial x} = -\frac{1}{\rho}\frac{\partial p}{\partial x} + v\frac{\partial^2 v}{\partial x^2} + v\frac{\partial^2 v}{\partial y^2} + v\frac{\partial^2 v}{\partial z^2} \tag{3}$$

$$Mz: \frac{\partial (\rho w)}{\partial t} + u\frac{\partial (\rho w)}{\partial x} + v\frac{\partial (\rho w)}{\partial x} + w\frac{\partial (\rho w)}{\partial x} = -\frac{1}{\rho}\frac{\partial p}{\partial x} + v\frac{\partial^2 w}{\partial x^2} + v\frac{\partial^2 w}{\partial y^2} + v\frac{\partial^2 w}{\partial z^2} \tag{4}$$

Where *Mx*, *My* and *Mz* are the momentum in *x*, *y* and *z* respectively and *P* is the pressure.

Energy equation:

$$\frac{\partial T}{\partial t} + u\frac{\partial T}{\partial x} + v\frac{\partial T}{\partial y} + w\frac{\partial T}{\partial z} = \frac{\lambda}{\rho Cp}\frac{\partial^2 T}{\partial x^2} + \frac{\lambda}{\rho Cp}\frac{\partial^2 T}{\partial y^2} + \frac{\lambda}{\rho Cp}\frac{\partial^2 T}{\partial z^2} \quad (4)$$

Where T is the amount of heat of the fluid, λ is the thermal conductivity and Cp is the specific heat of the fluid.

2.1 Geometric modeling at the tank inlet

Computational fluid dynamics is widely used in various researches, it uses computational resources to simulate problems related to fluid flow, for which it requires the use of physics, mathematics and programming tools to solve the problem, then generates the data to be further analyzed (Dhakal et al., 2015). To allow easy access to solutions from all commercial CFD packages, this tool includes modern interfaces for entering problem parameters and examining the results. Therefore, all codes contain three main elements: a preprocessor, a solver and a postprocessor (Versteeg and Malalasekera, 1995). Fig. 3 shows the geometry used in the simulation whose measurements were imposed according to a bibliographic review of simulations and more typical experimental benches, for both geometries the inlet is 1.5 m square and an unwrapping length of 7.5 m, the cylinder diameter is 5.5 m and the discharge diameter is 1.0 m.

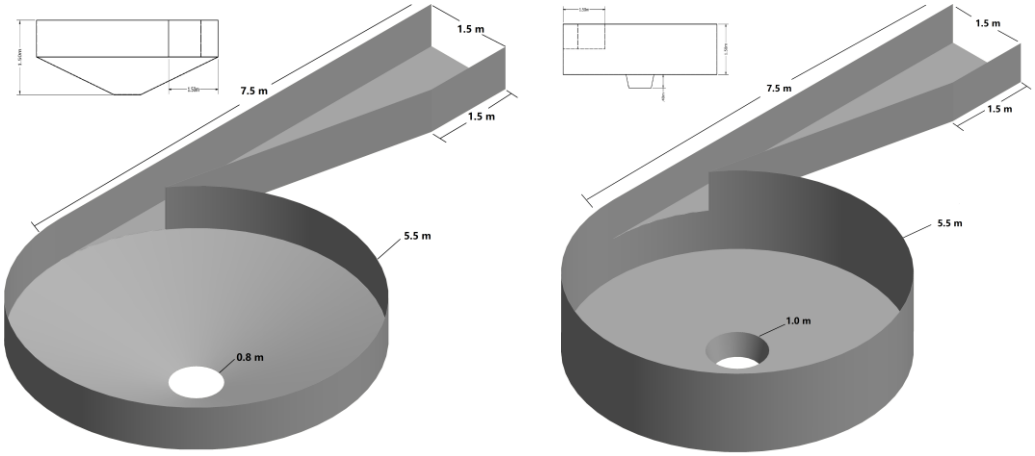

Figure 3. Geometry used for the simulation, conical (left) and cylindrical (right).

With these measurements, the geometry was modeled in Autodesk Inventor, which is compatible with ANSYS 2020 R1 software, and then exported to the program's geometric modeler. The entire control volume shown in Fig. 3 corresponds to the structure whose domain will be simulated to observe the phenomena that unfold. The program considers *Inlet* as the square face, *Outlet* as the discharge diameter of the tank, *Ambient* as the top of the tank and *Wall* as the faces of the tank body, whose material is concrete.

2.2 Mesh evaluation and fine-tuning

After performing the geometry in Autodesk Inventor of the domain, the meshing was performed using the ANSYS meshing tool. For the conical geometry the MultiZone method was used, this meshing method provides an automatic decomposition of the geometry into mapped regions and free regions, i.e., all regions are interlocked with a hexahedral mesh. For the cylindrical geometry two types of meshing were performed, for the inlet channel and discharge cone the MultiZone method was used and for the cylindrical tank the Automatic method was used, which is a default method and generates a mesh according to the geometry, it could be the case that it generates both tetrahedral and hexahedral meshes. The meshing of both geometries can be seen in Fig. 4.

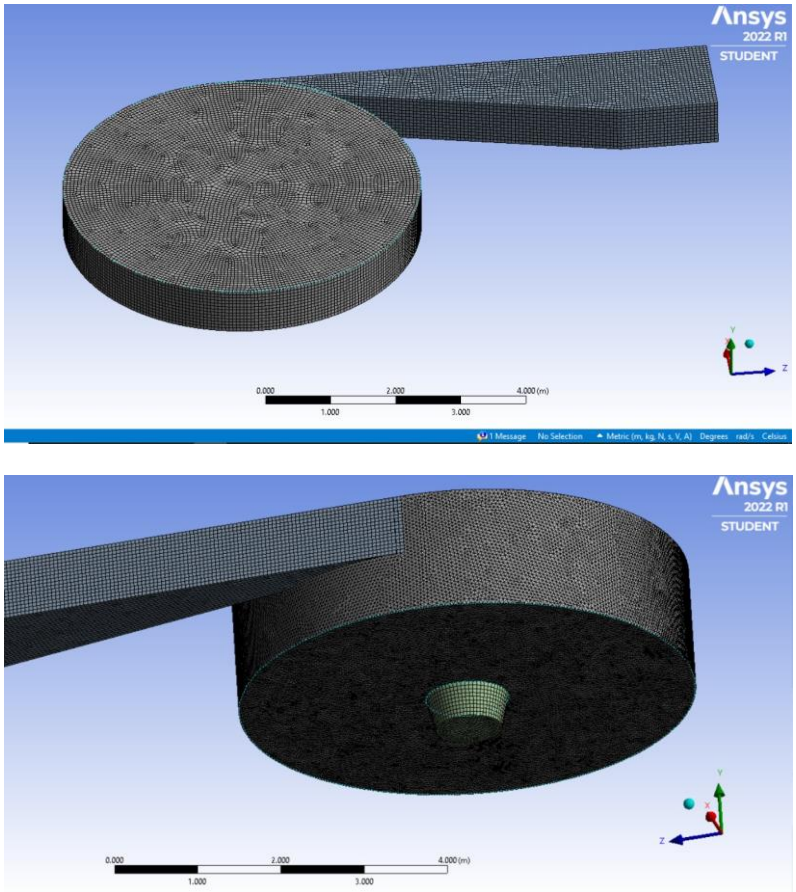

Figure 4. Geometry used for simulation, conical (top) and cylindrical (bottom).

The characteristics of the mesh quality were evaluated with the Orthogonality whose average orthogonal quality range varies from 0 to 1, being the first value an index of Low Quality and the second of High Quality, in our case we had for the conical and cylindrical tank values lower than 1; however, the conical mesh presents better quality. The aspect ratio obtained for the conical and cylindrical tank was 3.4352 and 1.7716, respectively, it is recommended that this maximum value be equal to 5 on average. These parameters are shown in Tab. 1., in addition to the number of nodes and elements for each type of geometry. In Tab. 2 shows the boundary conditions used in the numerical simulation for both tank geometries.

Table 1. Meshing information for both geometries

Characteristics	Conical Tank	Cylindrical Tank
Number of elements	485 346	2 668 764
Number of nodes	506 193	509 921
Orthogonality (Orthogonality)	0.60273	0.11192
Aspect Ratio (Aspect Ratio)	3.4352	1.7716

Table 2. Numerical boundary conditions for both geometries.

Conditions	Conical - Cylindrical Tank
Inlet	Subsonic/Normal Speed
Outlet	Subsonic/Opening Pressure
Turbulence model	k-Epsilon
Type of simulation	Steady-state
Phase type	Phase (Air and Water)

In this research, the Multiphase fluid model was considered as a homogeneous model, where water is the primary fluid. In addition, Heat Transfer, Combustion and Thermal Radiation will not be taken into account, since they are not of interest for our research. The turbulence model used is k-Epsilon.

The surface tension coefficient used for our model was 0.072 N/m, which allows us to place the air above the water within the studied domain. In addition, the Surface Tension Model, the Interphase Transfer and the Mass Transfer will not be taken into account, since they are not of interest for our research either. The medium turbulence intensity (Medium Intensity) recommended by ANSYS is 5% when industrial and engineering numerical simulations are required and no laboratory data are available to calculate the intensity.

The volume fraction of water is taken as 1 since only the mass flow of water is required, and the volume fraction of air in this case is 0 due to the previous condition.

2.3 Convergence and stability criteria

The balances by means of the equations evaluate the conservation of mass, momentum and energy throughout the simulation domain. According to Villarroel Quinde (2015), in a time step, the simulation is considered to be stationary so the balance results from subtracting the inflow with the outflow of the variable and dividing it by the maximum flow. In a simulation with ideal convergence, the inflow is equal to the outflow so the ideal balance would be 0%, then, a completion criterion for the balances of the flow variables is that they are below 1%. (ANSYS CFX, 2020).

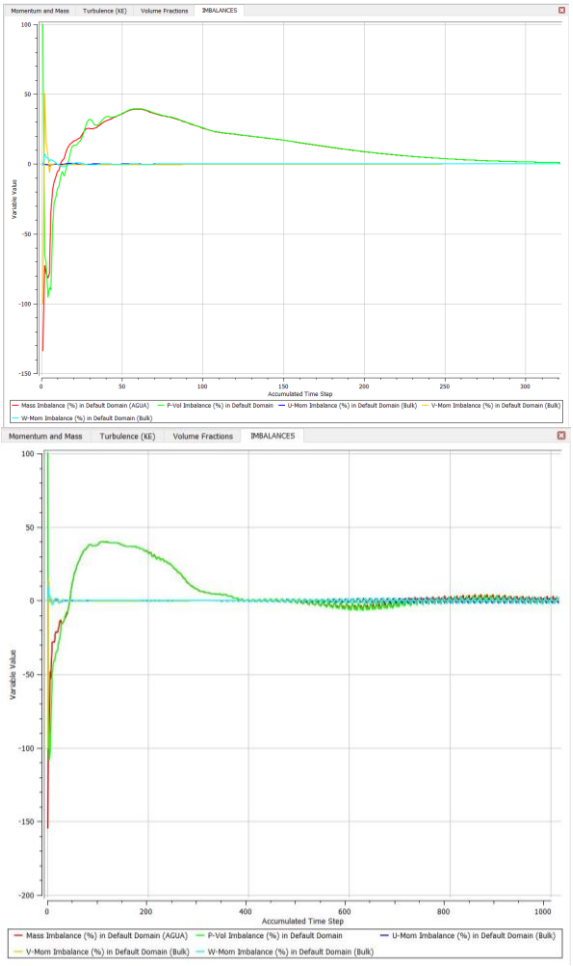

Figure 5. Evolution of imbalances as a convergence criterion, conical (top) and cylindrical (bottom).

For the validation of the simulation, the behavior of the balances as well as the conservation of mass throughout the system were evaluated. In Fig. 5 we can see that the mass and volume curves enter a domain in which no strong oscillations are perceived. In the top figure for the conical tank geometry, a convergence is observed from the cumulative time step of about 300 and in the bottom figure for the cylindrical tank geometry, the convergence is from the cumulative time step of about 400. In both cases, the balances of the flow variables are found to be 0.9811% and 0.5013%, respectively. For the conical and cylindrical geometry, these values are well below the imposed criterion of 1% and, from that, we can conclude that the rounding and interpolation errors are not significant and that the conservation of the flow variables is fulfilled.

3. RESULTS AND DISCUSSIONS

The results obtained by means of the simulation in ANSYS 2022R1 were for two tanks with conical and cylindrical geometries, in addition to the analysis of the behavior of the velocities developed inside the tank chamber. In Fig. 6 the velocity field for the conical geometry tank is presented, it can be observed that the velocity at the outlet of the discharge orifice is higher; however, to obtain a better performance it should be located in the vortex formation zone which is developed in the center of the tank, obtaining values close to 2.42 m/s approximately. The left side of Fig. 6 shows the formation of vortices and the right side shows the uniformity of the flow development inside the tank.

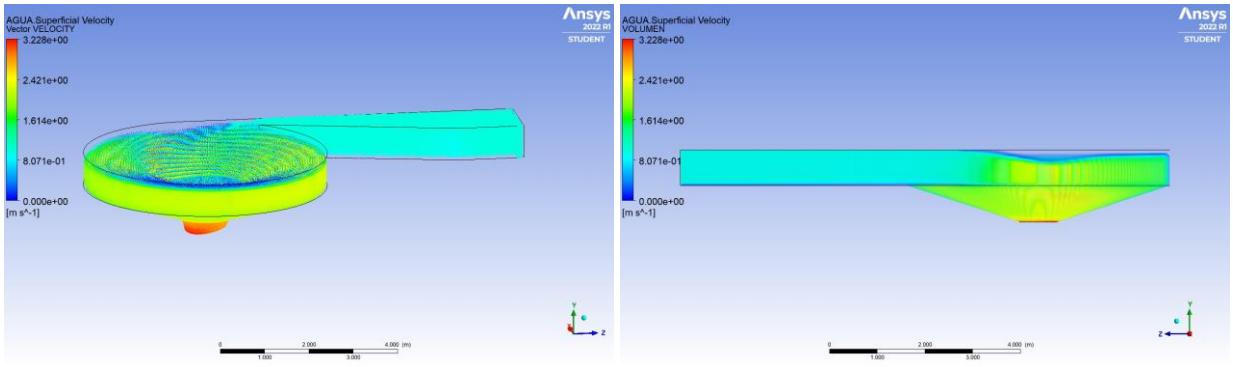

Figure 6. Velocity field for the conical type tank.

Fig. 7 shows the velocity field for the cylindrical geometry tank, the highest velocity is observed at the outlet of the orifice, as in the case of the conical tank; however, the relevance of the formation of gravitational vortices is precisely to take advantage of these eddies, finding that the speed in this case is approximately 1.85 m/s. In the left part of Fig. 7, a group of velocity vectors can be observed coming out of the tank contours in the upper part, this occurs due to an overflow phenomenon of the chamber, which should be evaluated in more detail in this type of geometry and in the right part of Fig. 7, the uniformity of the velocity field in the cylindrical tank is observed.

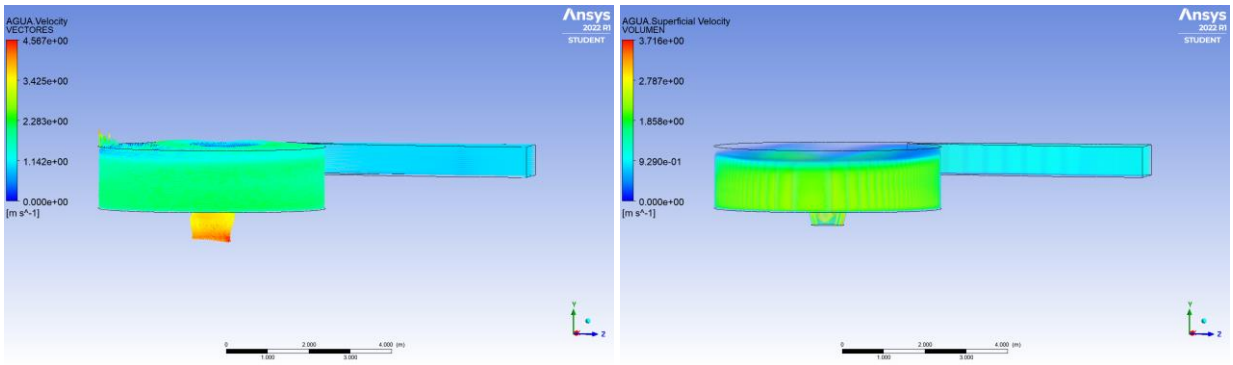

Figure 7. Velocity field for the cylindrical tank type.

For a better analysis of the fluid velocity field inside the tanks, a cross section of the conical tank was made using the homogeneous multiphase fluid model, as shown in Fig. 8 and Fig. 9. In these figures, the interface between air and water can be seen, and it can also be observed that the core of the vortex contains air inside, which helps to maintain a pressure in the water, becoming a favorable condition in the formation environment. The velocity profile in the radial direction shows a gradual increase in water velocity due to rotational eddying and potential energy conversion (Wanchat and Suntivarakorn, 2012).

It is important to note that for the conical tank geometry the surface velocity is in the range of 2.26 m/s to 2.58 m/s, shown in the yellow spectrum. On the other hand, for the cylindrical tank geometry the surface velocity is not so uniform, being in the range of 1.85 m/s to 2.23 m/s, being lower than in the conical tank. However, one aspect that has to be highlighted is that it does not present a constant velocity field, which can generate instabilities in the operation of the turbine.

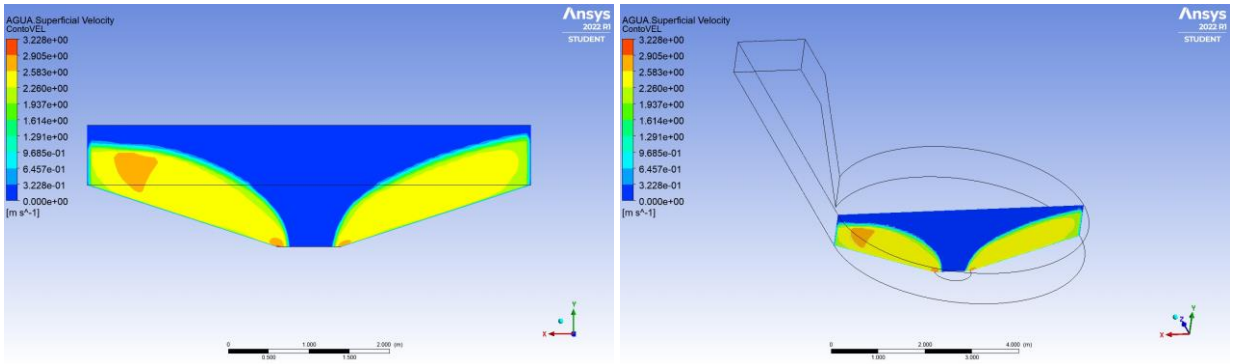

Figure 8. Velocity field for conical tank, center plane.

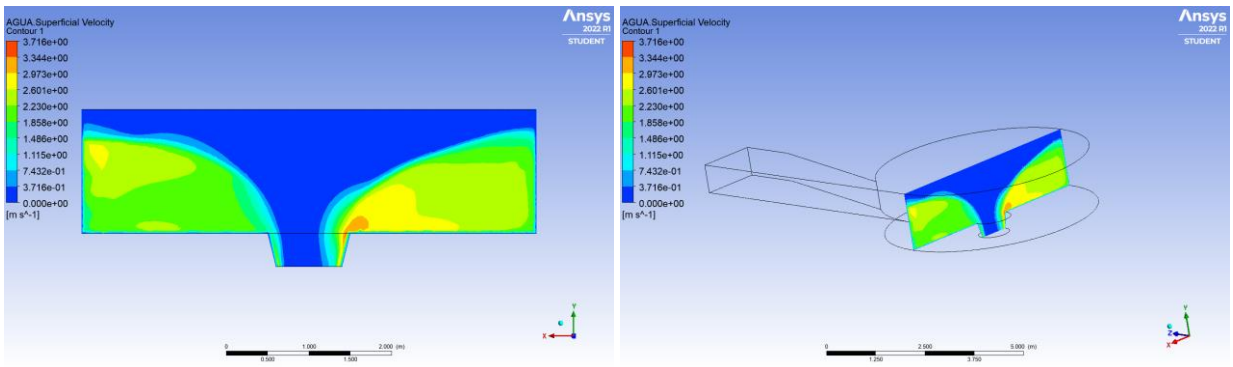

Figure 9. Velocity field for the cylindrical tank, center plane.

Based on these results, it is concluded that the tank with conical geometry could transfer more energy from gravitational vortex formation compared to the tank with cylindrical geometry. To improve these conditions, modifications to the tank dimensions should be evaluated, as well analyses the influence of the tank inlet angle. It should be noted that the geometric height or hydraulic jump available in the field should be an important parameter to be considered in the development of researches related to this study.

4. CONCLUSIONS

The In this research work, an evaluation of the influence of the geometry of the tank at the entrance that favors the formation of the gravitational vortex phenomenon has been carried out, two types of typical geometries were used in these energy generation systems, which are results in a first stage of investigation.

From the results obtained numerically, in the conical tank geometry, a convergence is observed from the cumulative time step of about 300 and in the bottom figure for the cylindrical tank geometry, the convergence is from the cumulative time step of about 400. In both cases, the balances of the flow variables are found to be 0.9811% and 0.5013%, respectively.

The results obtained were from the use of CFD to evaluate the behavior of the vortex, for the conical tank a speed of 2.42 m/s was obtained and for the cylindrical tank a speed of 1.85, approximately. These values vary in the domain, however, for the same evaluated point, it is concluded that the tank with a conical inlet offers better behavior in the formation of vortices.

5. ACKNOWLEDGEMENTS

The authors would like to thank the Cesar Vallejo University (UCV), National University of Santa (UNS) and National Council for Science and Technology (CONCYTEC).

6. REFERENCES

Adam Faraji, Yusufu Abeid Chande Jande and Thomas Kivevele, 2022. “Performance analysis of a runner for gravitational water vortex power plant”. *Energy Sciencie & Engineering*, Vol. 10 (2022), pp 1055-1066.

ANSYS CFX, 2020. “Reference Guide”, 12 Mar. 2022 <ANSYS Software - Simulación Computacional - ESSS> .

Arregui, F., Cabrera, E., Cobacho, R., Gómez, E., & Soriano, J. (2017). *Apuntes de mecánica de fluidos.* Universidad Politécnica de València, 4ta edición.

Céspedes J.C. and Saldaña J.S., 2021. Estudio de prefactibilidad para la producción de energía hidráulica renovable mediante generadores de vórtice gravitacional en canales del distrito Motupe. Thesis, Pedro Ruiz Gallo National University, Lambayeque, Perú.

COES. Estadística Anual 2020. Portal del Comité Económico del Sistema Eléctrico Peruano. 2021, 28 Mar <https://www.coes.org.pe/Portal/publicaciones/estadisticas/estadistica2020#>.

Dylan S. Edirisinghe, Ho-Seong Yang, S.D.G.S.P. Gunawardane and Young-Ho Lee, 2022. "Enhancing the performance of gravitational water vortex turbine by flow simulation análisis". *Renewable Energy*, Vol. 194 (2022), pp 163-180).

Gardea Villegas, H, 2001. "Conceptos básicos sobre la formación y teoría de los vórtices". *Ingeniería, Investigación y Tecnología*, Vol. II2, pp 81-87.

López, B., 2015. *Aplicación de CFD ANSYS FLUENT en el estudio hidrodinámico de tanques de recirculación empleados en acuacultura*. Tesis de Maestría. Universidad Autónoma del Estado de México, México.

Sagar Dhakal, Ashesh B. Timilsina, Rabin Dhakal, Dinesh Fuyal, Tri R. Bajracharya, Hari P. Pandit, Nagendra Amatya and Amrit M. Nakarmi, 2015. "Comparison of cylindrical and conical basins with optimum position of runner: Gravitational water vortex power plant". *Renewable and Sustainable Energy Reviews*, Vol. 48, pp 662-669.

Timilsina, A. B., Mulligan, S., & Bajracharya, T. R. (2018). "Water vortex hydropower technology: a state of the art review of developmental trends". *Clean Technologies and Environmental Policy*, Vol. 20(8), pp 1737–1760.

Versteeg HK, Malalasekera W., 1995. *An introduction to computational fluid dynamics*. In: Versteeg HK, Malalasekera W, editors. New York: John Wiley & Sons Inc.

Villarroel Quinde, L.F., 2015. *Simulación numérica de un flujo de agua a través de una válvula tipo mariposa de doble excentricidad*. M.Sc. Thesis, Pontifical Catholic University of Perú, Lima, Perú.

Wanchat S., and Suntivarakorn R., 2012. "Preliminary Design of a Vortex Poofor Electrical Generation". *Advanced Science Letters.* Vol.13, pp 173–177.

7. RESPONSIBILITY NOTICE

The authors are the only responsible for the printed material included in this paper.